12-1995

Improved periodic spectral analysis with application to diesel vibration data

Peter J. Sherman
Iowa State University, shermanp@iastate.edu

Lang B. White
Cooperative Research Centre for Robust & Adaptive Systems

Improved periodic spectral analysis with application to diesel vibration data

Peter J. Sherman
Iowa State University, Department of Statistics, Department of Aerospace Engineering & Engineering Mechanics, Ames, Iowa 50011

Lang B. White
Cooperative Research Centre for Robust & Adaptive Systems, Department of Defence, P.O. Box 1500, Salisbury, SA 5108, Australia

(Received 13 October 1994; revised 17 April 1995; accepted 22 May 1995)

The purpose of this work is to begin the development of a comprehensive time/frequency spectral analysis approach that can be applied to complex signals associated with real world systems, such as rotating machinery. Rotating machinery operating at nominally constant speed comprise a large class of important real world systems that have received relatively little attention in terms of stochastic characterizations of any greater sophistication than those associated with wide sense stationary processes. In this work, a periodic-time/frequency characterization procedure is introduced in the context of vibration analysis associated with a diesel engine operating at nominally constant speed. This application highlights a number of difficulties, such as the need for accurate period estimation, accommodation of noninteger periods in relation to digital processing, and identification and separation of tonal components from the signature in order to arrive at a more parsimonious characterization. A theorem relating to the limiting influence of these difficulties is presented. These difficulties are addressed using advanced signal processing tools, such as a recently developed tone identification procedure and extended Kalman filtering, which to the authors' knowledge have not been considered to date in such a setting. Results include a simple correction algorithm for noninteger periods, excellent separation of tonal components whose frequencies are slowly varying, and subsequently a modest improvement in the spectral characterization of the remainder of the process. These results have some significance in relation to diesel engine vibration, since they unambiguously identify tonal vibration components, in addition to a random structure which appears to include random excitation of resonances.

PACS numbers: 43.60.Gk, 43.40.Yq

INTRODUCTION

Periodic phenomena are found in a wide variety of disciplines. Examples include noise and vibration associated with rotating machinery, communication signals, pulsar signals, and species extinction rates. In view of the periodic nature of such phenomena, it is natural to assume that related signals may exhibit a periodic structure. For this reason, the frequency domain has been the predominant medium for attempting to describe the information contained in these types of signals. However, traditional frequency domain analysis assumes the signal to be wide sense stationary (WSS). If the signal is periodic and nonrandom, then this type of analysis will reveal the magnitudes (not the phases) of its Fourier series coefficients. The simplest example of this type of signal is a sinusoid, which in this paper will be also termed a tone. At the other extreme, if the signal is periodic and random, then this type of analysis will reveal an energy spectrum which need not reflect *any* information associated with the periodicity. A simple example of such a periodic random process is white noise, say $X(t)$, that is modulated by a square wave, say $w(t)$ with period T. The resulting process, $Y(t)=X(t)w(t)$ is periodic, or cyclostationary.[1] Even so, a lagged-product autocorrelation estimate will converge in probability to a Dirac delta function associated with an unmodulated white noise process. In both cases, the temporal description of the signal information over a period of the phenomenon is lost in the spectral estimate.

A number of methods which attempt to take direct advantage of known period information have been proposed. Order analysis involves sampling the signal at a rate proportional to the period, so that frequency bins are replaced by multiples of the period inverse. This technique has been used for decades in analysis of signals from rotating machinery. For a recent application, see Ref. 2. It is extremely valuable for accommodating slowly time-varying periods. For a constant period it becomes standard spectral analysis, and so provides no intracycle information. Synchronous averaging is a method whereby the data (or a simple function of it) is partitioned into blocks, the length of each which equals the known period, and these blocks are averaged.[3] In the frequency domain, this is equivalent to applying a comb filter. While this method is designed to extract a description of the intracycle information, it is very sensitive to bias and variability of the signal period. Moreover, it provides no time-varying frequency description of the data.

It may be argued that, in spite of the availability of advanced signal processing tools, there is no one tool which is sufficiently general to conduct a comprehensive time/

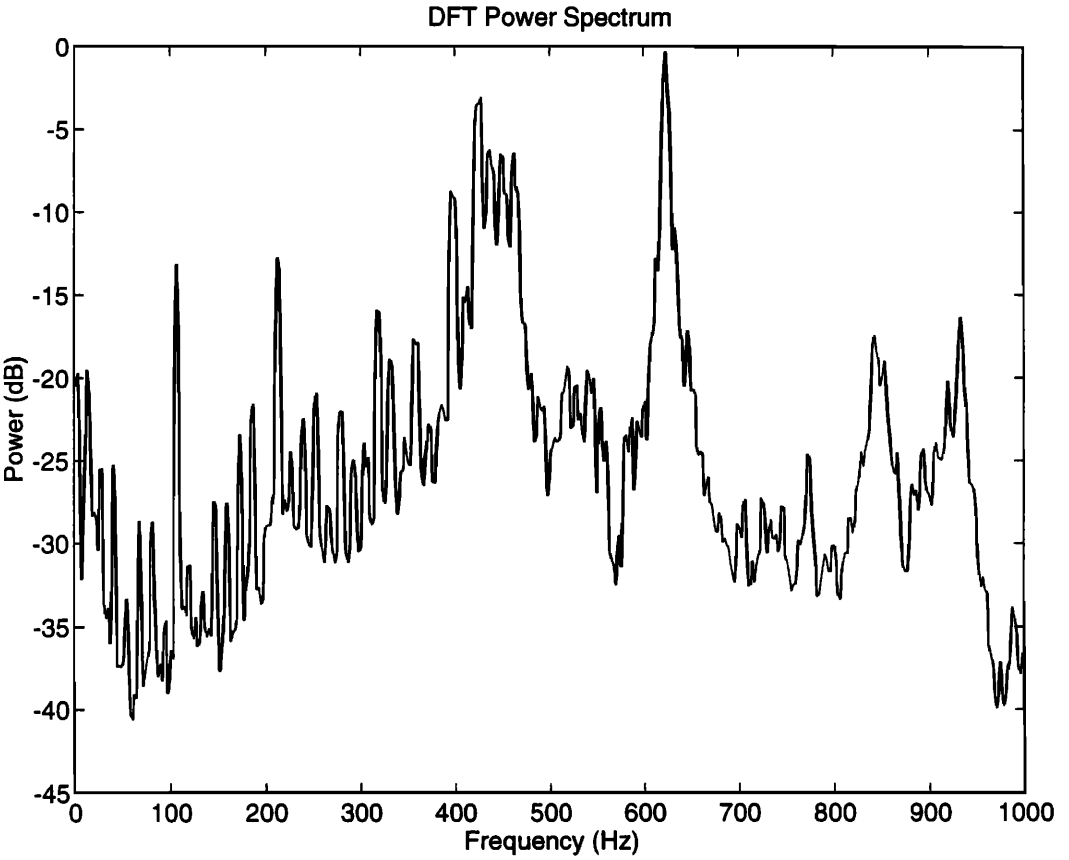

FIG. 1. Diesel data power spectrum estimate obtained by averaging thirty-two 1024-point spectra.

frequency analysis of stochastic processes associated with complicated real world systems such as rotating machinery. The goal of this work is to investigate the potential of a combination of advanced signal analysis tools for extracting periodic time-varying spectral information from real world data; that is, data associated with a nominally periodic phenomenon, and whose stochastic description is entirely unknown. For this purpose, vibration data obtained from an automotive diesel engine run at relatively constant speed will be the focus of this work. These data are believed to be suitably complex as to be representative of data associated with a wide variety of rotating machinery. It will provide the motivation to address a number of real issues, most notably time-varying period tracking and tone rejection. The signal processing tools needed to address these issues are described, and their performance is demonstrated in simulations, as well as in the case of the diesel data. The remainder of this work is organized as follows. Section I describes the diesel data collection procedure. Section II reviews elements of spectral estimation for *wss* processes, and includes a number of such estimates for the diesel data. The presence of sharp peaks in the spectral data (as is almost always the case in rotating machinery data) motivates the search for the presence of point spectrum associated with tones. This is done in Sec. III, using a recently developed method for identifying sinusoids in unknown noise,[4] which can even be nonstationary,[5] as will be the case with the diesel data. Section IV includes a brief review of periodic random processes. Section V addresses period estimation and the influence of period uncertainty, in the form of bias and variability, on periodic spectral estimates. This is a particularly important problem, since in many real world situations both inexact period information is provided, and load variations are present which can induce small random fluctuations. The effect of these fluctuations is described in a theorem, which states that the limiting structure of any periodic spectrum estimate, in the case where the assumedly constant period is in fact a stationary random process, becomes time-invariant. Section VI addresses the problem of tone removal. Tones are often contained in random processes associated with rotating machinery. Tone removal is important in periodic spectrum estimation, since in the time frequency plane a tone is time invariant. Hence, its presence not only reflects redundant information, but it can camouflage the time-varying spectral structure of other processes. To achieve tone rejection (the need for which is highlighted by the diesel results of Sec. IV) an extended Kalman filter (EKF) is proposed, and its performance is evaluated. Finally, Sec. VI includes a summary of our proposed approach for periodic spectrum analysis of data associated with periodic phenomena, and draws conclusions regarding its value and limitations. Issues for further research are also identified.

Before proceeding to Sec. I, the reader should be warned that the style of this paper is not the traditional one of presenting all of the analytical machinery first, and then demonstrating its utility in an application. While such an approach

has its place, it can intimidate the practitioner who does not have the patience to wade through all of the prerequisite material. Moreover, it is seldom the way in which the research actually evolved. This is especially true in this work. We intentionally chose to let the real world problem, in this case the desire to obtain a time/frequency description of diesel engine vibration, drive the effort. Consequently, our presentation approach is to reflect this. For this reason, the reader will find analyses and figures related to the diesel engine vibration analysis throughout the paper. While this may result in some inconvenience, for example in comparing figures, we believe that it has the advantage of providing needed continued practical motivation throughout the paper.

I. DIESEL DATA COLLECTION

Vibration data from a 6.2-L, 8-cylinder automotive diesel engine were collected while the vehicle was operated at a speed of 55 miles per hour (mph) on a flat highway with negligible wind conditions. Cruise control was use to attempt to maintain speed as constant as possible. An accelerometer was magnetically mounted on the valve cover above the number 1 cylinder. The analog vibration signal was run through an anti-aliasing fifth-order Bessel low-pass filter with a cutoff frequency of 500 Hz. Digitization was performed at a rate of approximately 2000 samples/second. A total of 32 768 samples were collected continuously over a period of approximately 16 s. Based on speedometer observations, the vehicle speed fluctuated by no more than ± 1 mph.

II. TRADITIONAL SPECTRAL ANALYSIS

A discrete Fourier transform (DFT) power spectrum estimate [cf. Eq. (1) below] of the diesel data is shown in Fig. 1. It was obtained by averaging 32 individual (modulus squared) DFTs of data records of size 1024. The presence of peaks spaced apart an amount equal to the engine shaft frequency of approximately 13.1 Hz (the bin width is ~ 1 Hz) is characteristic of DFT spectra derived from rotating machinery data. The first large peak at ~ 105 Hz corresponds to the first cylinder harmonic. The relatively large peaks at the cylinder harmonic frequencies identified in this figure reflect, in part, the similarity of the signals associated with the individual cylinders, in spite of the proximity of the sensor above the number one cylinder. Analysis of this vibration spectrum suggests that a broad resonance just above 400 Hz is being excited by the fourth cylinder harmonic and neighboring shaft harmonics, while a narrow resonance is being excited, possibly by the sixth cylinder harmonic and neighboring shaft harmonics. Such an analysis however, requires qualification. Specifically, are these resonances (if they are indeed resonances) being excited primarily by sinusoids (termed tones in this work) or by random narrow-band energy sources. This distinction is important, If they are excited by tones, then the peaks in question represent power, and Fig. 1 is a valid approximation of the theoretical line structure associated with a power spectrum. In this case, the portion of Fig. 1 which does not contain peaks suggestive of line spectrum is, in a sense, meaningless, since its amplitudes are controlled by the size of the records (in this case, 1024) used to compute the DFT. To see this, recall that the power spectrum associated with a wide sense stationary zero mean random process, X_t, is given by

$$P_x(\omega)=\lim_{N\to\infty}\frac{1}{2N}\sum_{\tau=-N}^{N}R_x(\tau)e^{-i\tau\omega}, \tag{1}$$

where $E(X_t,X_{t+\tau})\triangleq R_x(\tau)$ is the autocorrelation function. If $X_t=A\sin(\Omega t+\phi)$, where ϕ is uniformly distributed over $[0,2\pi]$, then $R_x(\tau)=(A^2/2)\cos(\Omega\tau)$ and (1) will converge to zero at every frequency except $\pm\Omega$, where it will exhibit a line with height $\pm A^2/4$.

If X_t is white noise, then $R_x(\tau)=\sigma_x^2$ for $\tau=0$ and is zero for $\tau\neq 0$, so that (1) converges to zero everywhere. For this type of random process the appropriate spectral quantity is the energy spectrum, given by

$$S_x(\omega)=\lim_{N\to\infty}\sum_{\tau=-N}^{N}R_x(\tau)e^{-i\tau\omega}. \tag{2}$$

For white noise, (2) converges to σ_x^2. In practice, especially when studying processes associated with real world periodically excited systems, such as rotating machinery, the estimated spectrum will contain a mixture of line spectrum and continuous spectrum. This mixed spectrum identification problem is discussed in Ref. 6. Suffice to say, the crux of the problem is to determine which peaks in a spectral estimate correspond to (1) and which correspond to (2).

One possible solution to this problem is to compute a family of DFT spectra indexed by the number of autocorrelation lags used. Alternatively, a family of autoregressive (AR) spectra might be utilized, since it is well known that they can offer notably higher tone resolving properties than the DFT for the same number of lags. Let $\mathbf{X}_t=[X_{t-1},\ldots,X_{t-n}]^{tr}$ and let $\mathbf{a}=[a_1,\ldots,a_n]$ be the vector of linear prediction parameters which minimize the expected squared prediction error $\sigma_e^2\triangleq E(X_t-\mathbf{a}\mathbf{X}_t)^2$. Then the corresponding AR(n) spectral estimate, which relies on $\{R_x(\tau)\}_{\tau=0}^{n}$, is given as

$$AR_n(\omega)\triangleq|\sigma_e/[1,-\mathbf{a}]\mathbf{w}(\omega)|^2, \tag{3}$$

where $\mathbf{w}(\omega)\triangleq[1,e^{-i\omega},\ldots,e^{-in\omega}]^{tr}$. The diesel data AR($n$) spectral estimates for $n=20$, 40, 80, and 160 are shown in Fig. 2. One can use any one of these spectra as an energy spectrum estimate. One could also use all of them to determine, from their behavior as a function of n, which frequencies correspond to tones. Specifically, because (3) is an estimate of (2), then as $n\to\infty$, peaks in (3) at tone frequencies will become unbounded. For example, in Fig. 2 the peaks corresponding to the first, second, and fourth cylinder harmonics all appear to increase as a function of n, while the one at the sixth harmonic (622 Hz) appears to have little dependence on n. From this, one might conclude that of these harmonics, only the sixth corresponds to a narrow-band energy, as opposed to a tone source. We now discuss the use of a different family of spectra for this purpose.

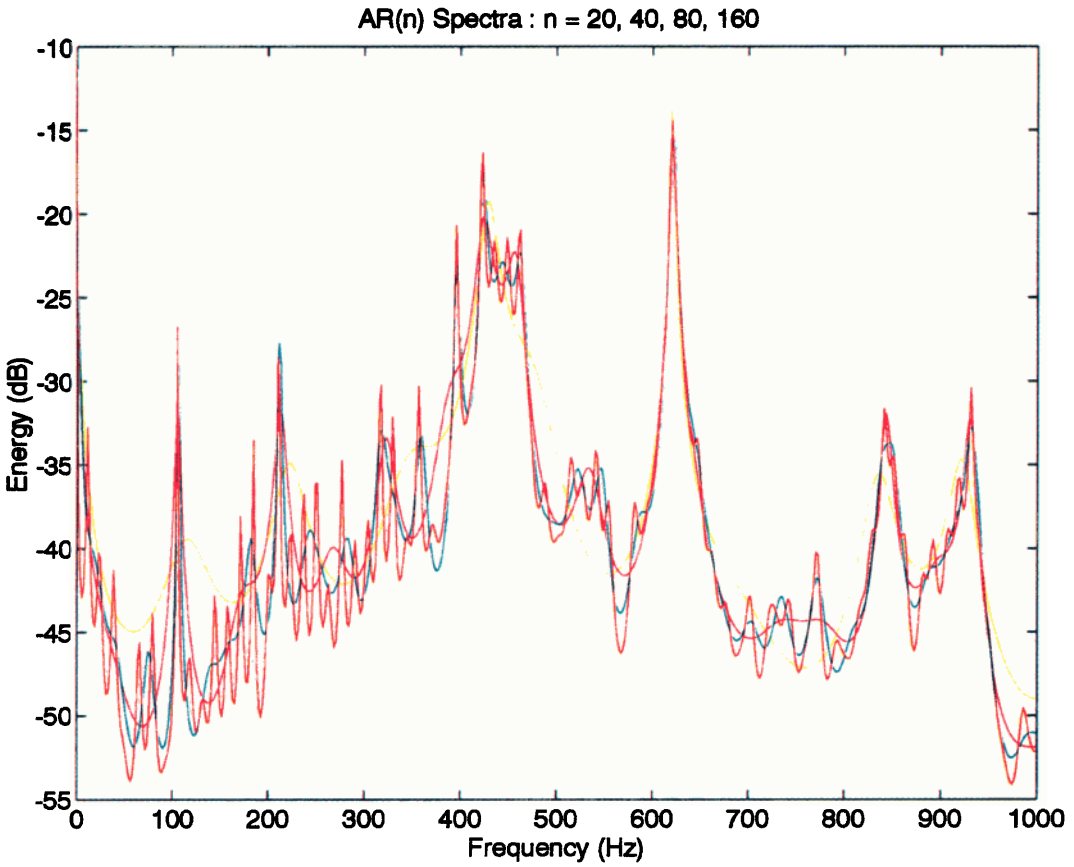

FIG. 2. Diesel data AR (n) spectral estimates for $n=20$ (yellow), 40 (red), 80 (blue), 160 (orange).

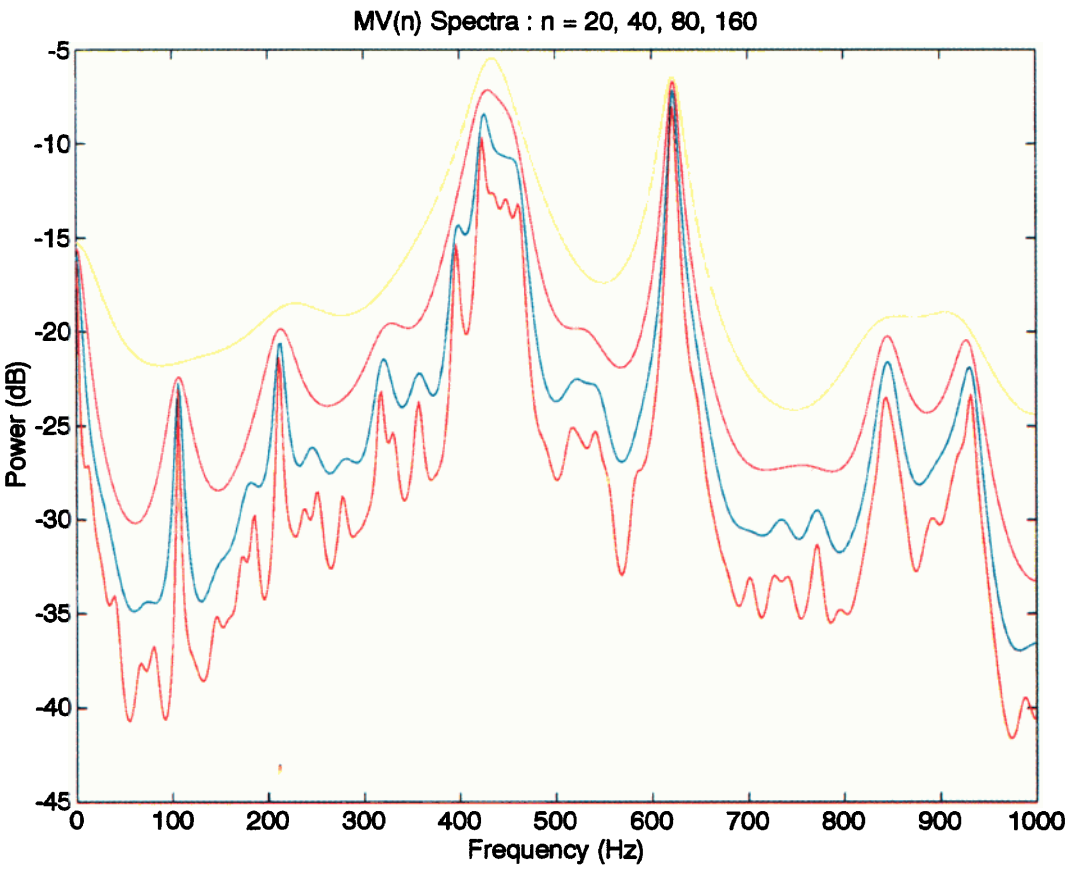

FIG. 3. Diesel data MV (n) spectral estimates for $n=20$ (yellow), 40 (red), 80 (blue), 160 (orange).

III. IDENTIFICATION OF TONES USING THE FAMILY OF MINIMUM VARIANCE SPECTRA

In DFT-based spectral analysis the only difference between a power (1) versus an energy (2) spectral estimate is a factor of $1/2N$. For example, note the similarities between the AR(160) energy spectrum in Fig. 2 and the DFT power spectrum in Fig. 1; the difference in scale being $1/2(512) \cong 30$ dB. An exception to this difference however, is apparent at the first two cylinder harmonics, where tones predominate. In these regions the amplitudes of the peaks in the AR(160) spectrum are meaningless.

In the last section the use of a family of spectral estimates, specifically AR(n) spectra, indexed by n, the number of autocorrelation lags utilized, was suggested as a means of identifying tones. The problem with using AR(n), as well as associated DFT spectra, for this purpose is that the growth rate of a peak as a function of n can be quite erratic, making it difficult to draw conclusions regarding convergence. The following family of minimum variance (MV) spectra overcome this difficulty to a notable extent. The MV(n) spectrum for a scalar process X_t is

$$\mathrm{MV}_n(\omega) \triangleq \left(\sum_{k=0}^{n} \mathrm{AR}_k(\omega)^{-1} \right)^{-1}. \tag{4}$$

The MV(n) spectrum was introduced as a power spectrum estimate by Capon[7] in 1969. Only recently, however, have its convergence properties as a function of n been exploited for identification of tones.[4,6,8] The diesel data MV(n) spectra for $n=20$, 40, 80, and 160 are shown in Fig. 3. Not only do the MV(n) spectra converge monotonically downward to the process power spectrum, but at each frequency where there is no line spectrum they drop at an asymptotic rate of 3 dB per doubling of n.[6] With this in mind, a visual inspection of Fig. 3 provides strong support for the tone nature of the first two cylinder harmonics. While the peaks in the 400- and 600-Hz regions drop notably more slowly than the asymptotic 3 dB per doubling of n, the evidence for the presence of tones in these regions is less conclusive; even though using the convergence test proposed by Lyon and Sherman[9] they are identified as tones.

These tonal components need to be removed from the data prior to performing any type of time-varying spectral analysis. Otherwise, they will contribute time-invariant spectral peaks that could dominate any time-varying spectra in neighboring frequency regions; behavior which will be demonstrated in the next section.

IV. PERIODIC TIME-VARYING SPECTRAL ANALYSIS

This section summarizes some basic definitions and results for periodic processes. We then present a periodic spectral estimate for the diesel data. Its relatively time-invariant behavior is noted, motivating the investigation of the influence of period uncertainty provided in the next section. To begin, a random process X_t is said to be a (weakly) periodic process if both its mean $E(X_t) \triangleq \mu_x(t)$ and autocorrelation $E(X_t X_{t+\tau}) \triangleq R_x(t,t+\tau)$ are periodic functions of the variable t. Such processes are also termed wide sense cyclostationary (WCS), and we will refer to them as such in this work. There has been a notable amount of attention given to such processes. The majority of it has concerned representation theory, while a lesser amount has focused on data-related issues (see, for example, Ref. 10 for a recent survey of the area). A fundamental result along these latter lines, due to Pagano,[10] is that the autocorrelation function estimator given by

$$\hat{R}_x(t,t+\tau) = \frac{1}{N} \sum_{n=0}^{N-1} X_{t+nT} X_{t+\tau+nT} \tag{5}$$

converges in the mean-square sense to $R_x(t,t+\tau)$ as $N \to \infty$ when X_t is a regular wcs process with period T. By regular we mean, loosely, that X_t has only continuous spectrum for each t in $[0,T]$. The definition of a time-varying spectrum used in this work is

$$S_x(t;\omega) = \sum_{-\infty}^{\infty} R_x\left(t-\frac{\tau}{2}, t+\frac{\tau}{2} \right) e^{-i\omega\tau}. \tag{6}$$

The spectral analysis of the last two sections implicitly assumed the diesel vibration data to be WSS. The justification for this assumption is entirely valid for the DFT spectral analysis, due to the manner in which the 1024-point blocks of data were collected. To see this, suppose the beginning of the first block coincides with the shaft top dead center position. Then, assuming the diesel shaft period is 152 points (as will be argued in the next paragraph), the beginning of the second 1024-point block will coincide with the 113th point of the seventh period, the beginning of the third will correspond with the 73rd point of the 14th period, and so on. If one views this data collection as repeated collection of one period of a periodic-T random process, but with the start of the collection, say t_0, having a uniform distribution over $[0,T]$, then in fact the periodic process becomes a WSS process.[12] The AR spectral analysis is another matter, since only one long realization of X_t was used to compute a lagged-product autocorrelation function estimate. In this case, the question of wide sense stationarity remains unresolved, since there is no implicit assumption of how realizations would be collected with respect to the start of a period. The MV spectral analysis, which uses the same autocorrelation information as the AR analysis, remains valid, due to the fact that, as noted in Sec. III, this convergence-based method of line spectrum estimation permits the nontonal portion of X_t to be nonstationary.[5] In this section our analysis will involve partitioning the diesel data so that the start of each block coincides with the same point relative to the shaft top dead center position. In this case, X_t cannot be assumed to be WSS. The WCS assumption corresponding to (5) is, however, reasonable.

Our first time-varying spectral analysis of the diesel data utilized shaft period estimate of $T_{\text{shaft}} = 8/105 = 0.076$ s, where the cylinder frequency, $\hat{f}_{\text{cyl}} = 105$ Hz, was estimated from Fig. 1, and the factor of 8, reflects the eight-cylinder nature of the engine. At a sample rate of 2000 Hz, this corresponds to a true period $T_{\text{true}} = 152.38$ points. The closest integer-valued computation period is $T = 152$. Rather than computing the estimate (5) for this T and a large number of τ values, and then applying the discrete version of (6), which

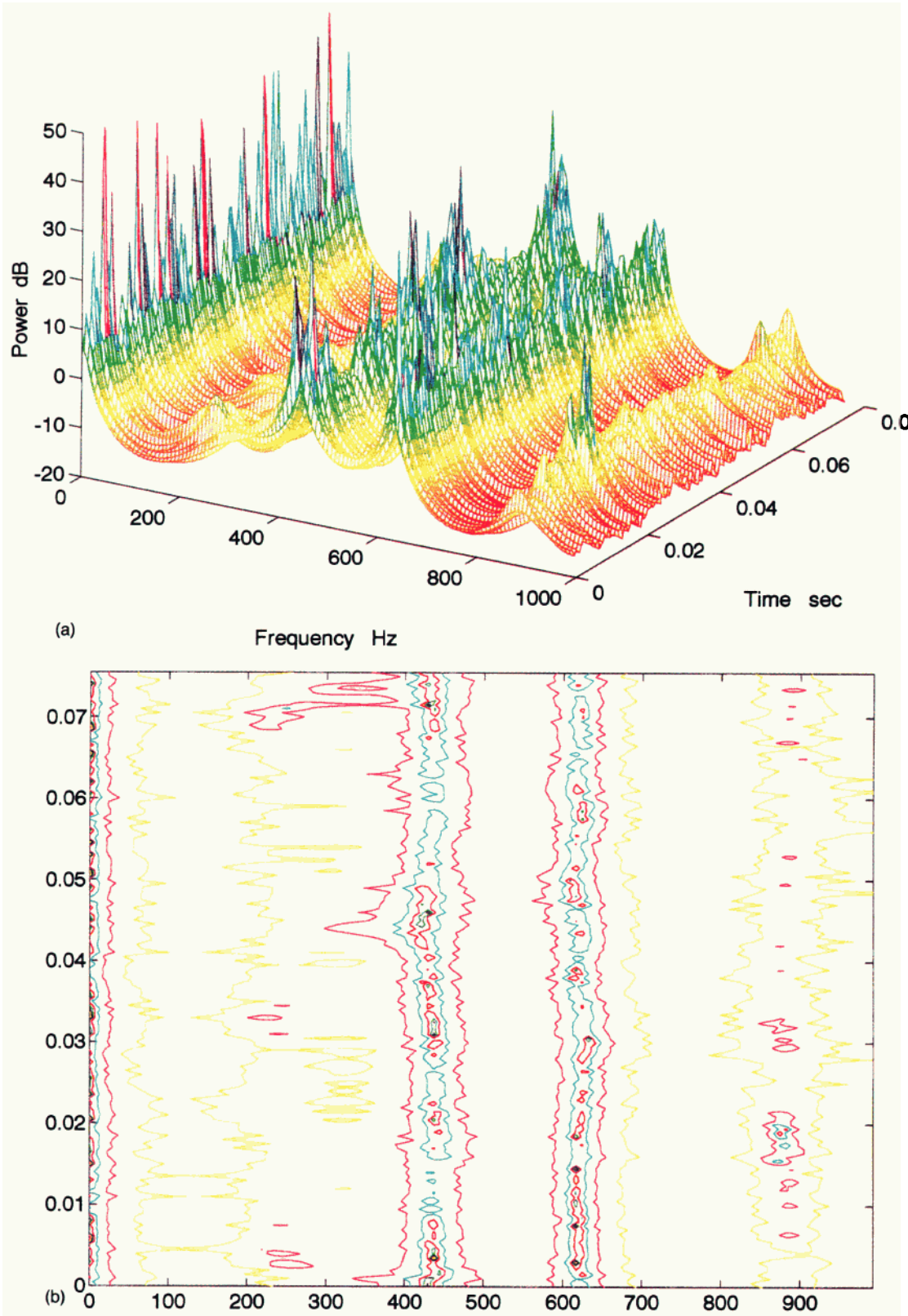

FIG. 4. Diesel data periodic time/frequency AR(10) spectral estimate using 262 periods of data at 152 points per period. (a) 3D plot, (b) contour plot.

amounts to a DFT-type periodic spectral estimate, it was decided to compute an AR-type periodic spectral estimate. The reasons for this decision are similar to those given for the case of spectral analysis of WSS data; namely a more parsimonious and computationally efficient estimate with potentially higher resolution.

A discrete-time random process X_t is said to be a WCS AR(p) process with period T, if for each $t=1,2,\ldots,T,X_t$ has an AR(p_t) representation with predictor vector $\mathbf{a}_t=[a_1(t),a_2(t),\ldots,a_{p_t}(t)]$ and white noise variance σ_t^2, where both the predictor vector and noise variance are periodic with period T, and $\mathbf{p}=[p_1,\ldots,p_T]$. Periodic AR models

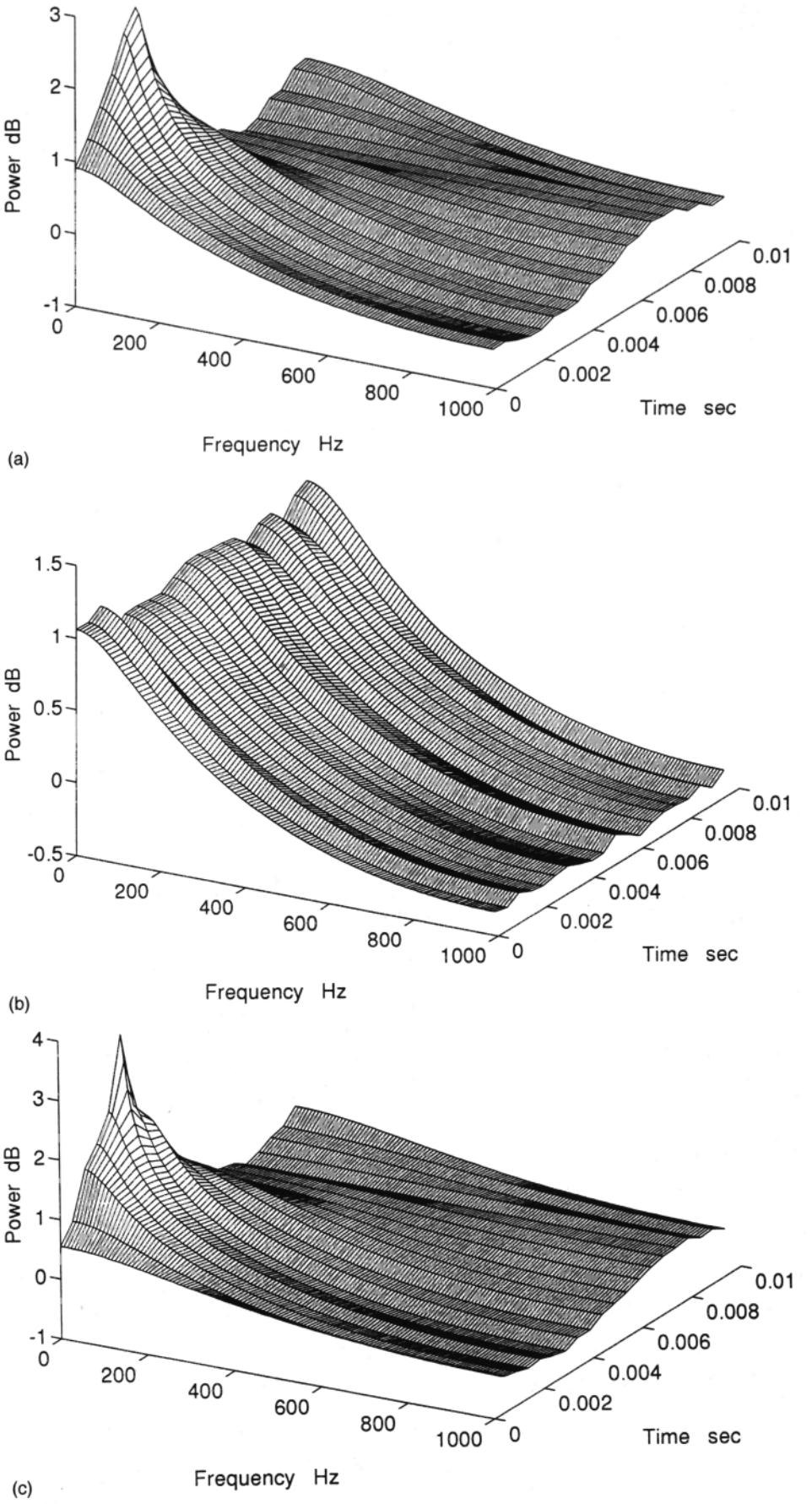

FIG. 5. AR(1) spectral estimates of the process given by Eq. (7), including (a) $T_{\text{true}}=T=20$, where T_{true} is the true period and T is the computation period; (b) $T_{\text{true}}=20.2$ and $T=20$; and (c) same as (b) but with the period correction scheme described in Sec. V applied.

form a special subclass of more general time-varying AR models which have been applied to rotating machinery problems.[13] They are also a subclass of a larger class of periodic random process models known as correlation AR processes,[14,15] which have also been applied to a rotating machinery problem in Ref. 13.

For a recent comprehensive summary of estimation of parametric models for WCS processes, see Ref. 16. In this work we use a least-squares approach for estimation of $\mathbf{a}_t$. This, as well as the estimate (5), involves partitioning the data into blocks of length T. Using the integer value of $T=152$, we have 215 periods of data available for estimation of the AR parameters. In this work, the AR order for each t was chosen to be 10. This was arrived at by studying variations in spectral estimates up to order 20, and noting little statistically reliable change in spectral structure beyond order 10. In general, one would implement an identification scheme, such as Akaike's final prediction error,[17] for each time throughout the period. This is currently under investigation.

The AR(10) periodic time/frequency spectral estimate of the diesel vibration data is given in Fig. 4. Throughout this work, both 3-D and contour plots of periodic spectral estimates are provided for ease of interpretation. While some time dependence is evident in Fig. 4, most notably in stronger peaks in the 400-Hz region around the time $t=0.03$, the spectrum exhibits a notable time-invariant structure.

V. THE INFLUENCE OF PERIOD UNCERTAINTY

The relatively time-invariant structure in Fig. 4 may be, in part, valid; especially in view of the suggestion of tone components provided by Fig. 3. However, the inaccuracy in our use of $T=152$ points per period, as well as period variations may also play a role. By ignoring the difference between the "true" and computed periods, $152.38-152=0.38$, then for a diesel data length of 32 768 the beginning of the last computed period will actually be located at $0.38(32\,768/152)\simeq 82$ points, or approximately one-fourth of a period preceding the start of the actual period. This type of precession of the computed period will have the effect of smearing the time-varying spectral structure of the data across the period. To demonstrate this consider the periodic AR(1) process

$$X_t=a_tX_{t-1}+e_t;\quad a_t=0.5+0.4\,\sin(2\pi t/T_{\text{true}}), \tag{7}$$

where e_t is a WSS white-noise process. Using 10 000 samples of (7) the AR(1) spectrum was estimated for $T_{\text{true}}=20$ and for $T_{\text{true}}=20.2$, while in both cases $T=20$. These spectra are shown in Fig. 5(a)–(b). These figures illustrate an interesting consequence of period bias on periodic spectral estimation, namely that unless it is accommodated, it can result in a time-invariant spectral estimate. In fact, in the case of integer-valued periods, it can be shown that if the computed and true periods are relatively prime, then the autocorrelation estimate, (3), will converge to a time-invariant one-dimensional autocorrelation. We now propose a method to accommodate this type of period bias.

Assuming a true and fixed period T_{true} is known, and the difference between it and the closest integer-valued computation period T is $T_{\text{true}}-T\triangleq\Delta$, then it is a simple matter to accommodate this difference. Specifically, let $\mathbf{X}_n=[x_{nT+1},x_{nT+2},\ldots,x_N]$ be all of the remaining data after the nth block. Beginning with $n=1$, partition the original data until the condition $n\Delta>0.5$ is noted. This implies that the beginning of the computed $(n+1)$st period is at least 0.5 samples behind the true $(n+1)$st period. Correct this condition by discarding the first point in $\mathbf{X}_n$, and proceed to partition this remaining modified data. If the condition $n\Delta<-0.5$ occurs, then a sample point needs to be added. This can be done in a number of ways. For simplicity we chose to add the average of x_{nT} and x_{nT+1} to the beginning of $\mathbf{X}_n$. The result of applying this fractional period correction scheme is demonstrated in Fig. 5(c). Comparison with Fig. 5(a) indicates that it is able to accommodate a fractional period with minimal distortion to the periodic spectral estimate.

The result of applying this period correction method to the diesel data is shown in Fig. 6. A comparison of Figs. 4 and 6 suggests that the proposed period correction scheme had a mixed effect on the time-varying nature of the spectral estimate. In particular, it diminished some temporally local peaks in Fig. 4, while accentuating others in the 400- and 600-Hz regions.

While the above period correction scheme may forestall the influence of period bias on the time-varying structure of a periodic spectral estimate, there is yet another period related phenomena, namely period variability, which can have the same effect. Period variability can be caused by load variations, combined with limitations in speed control systems. In the case of the diesel vibration data, speed variations on the order of ± 1 mph were observed. These could relate to load variations caused by small grade changes in the road, combined with the limitations of most cruise control systems. We now present a theorem which predicts the time invariant behavior of (5), hence time invariance of the spectral information, when an assumedly constant frequency $\Omega=2\pi/T$ is in fact a stationary random process $\Omega(t)$.

Theorem: Let $x(t)$ be the output of a time-periodic system $h(t,\tau)=h(t+T,\tau)$ excited by a WSS random process, $u(t)$:

$$x(t)=\sum_{\tau=0}^{M} h(t,\tau)u(t-\tau), \tag{8a}$$

where $h(t,\tau)$ has an absolutely summable Fourier series in t given by

$$h(t,\tau)=\sum_{q=-\infty}^{\infty} h_q(\tau)e^{iqt\Omega}. \tag{8b}$$

Then $x(t)$ is a periodic random process, and the autocorrelation estimate given by (5) converges in the mean sense to the corresponding two-dimensional autocorrelation function. If, on the other hand, in (8b) the process frequency Ω is a strongly stationary random process, $\Omega(t)$, then (5) converges in the mean to a one-dimensional autocorrelation function associate with a WSS process. In particular,

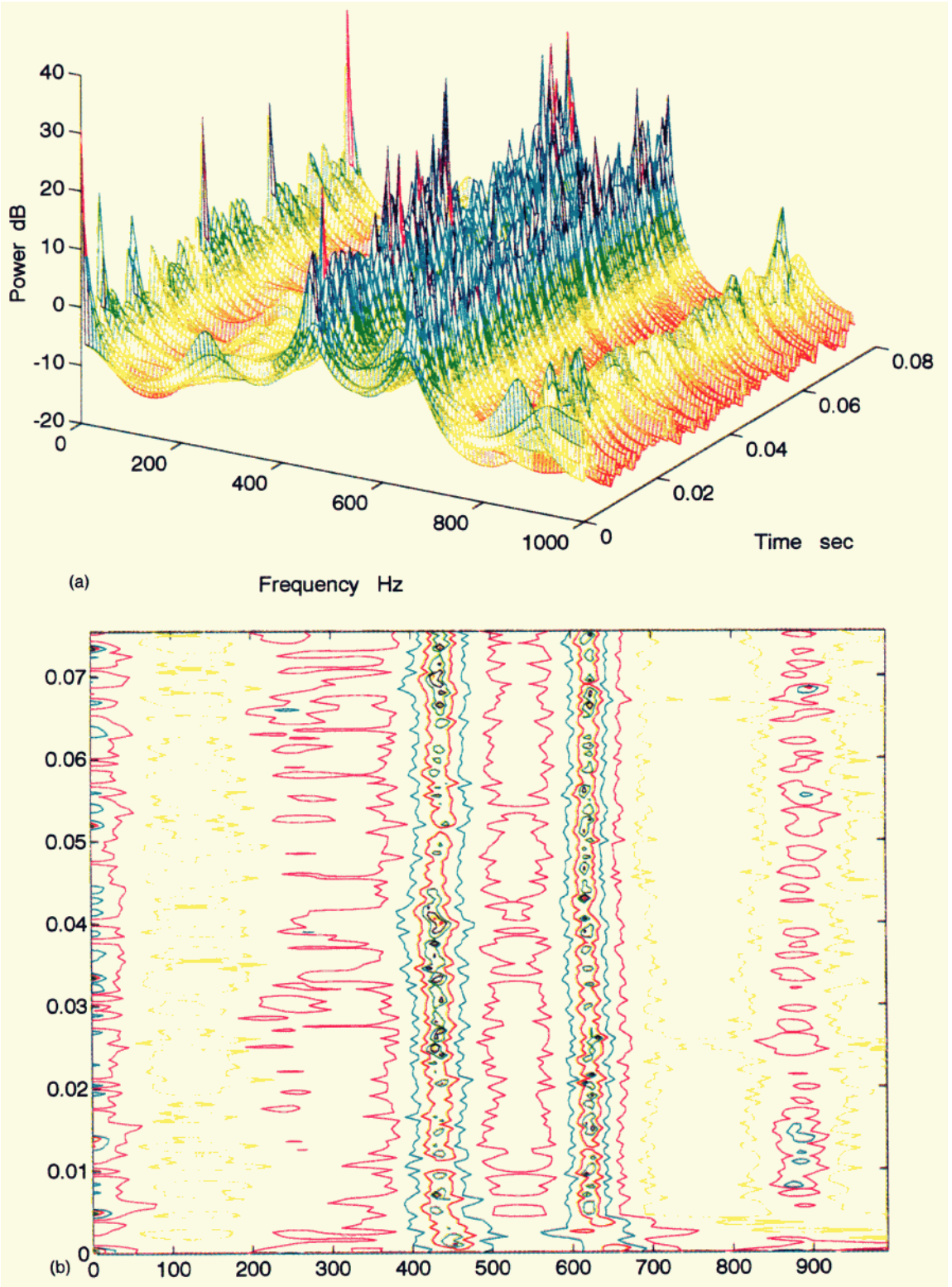

FIG. 6. Diesel data AR(10) periodic spectrum estimate using period correction under the assumption $T_{\text{true}}=152.38$ points/period and computation period $T=152$ points/period. (a) 3D plot, (b) contour plot.

$$\lim_{N\to\infty} E\,[\hat{R}_x(t,t+\tau)]=\sum_{\nu=0}^{M}\sum_{\eta=0}^{M} h_0(\nu)\bar{h}_0(\eta)R_u(\tau+\nu-\eta) \tag{8c}$$

is independent of t.

The proof of the theorem is given in Appendix A. Practically speaking, it points to the need to balance the amount of smearing of nonstationary structure with the statistical stability of the periodic spectral estimate. Both of these increase with the amount of data used.

Example: As an example, consider a quasiperiodic mov-

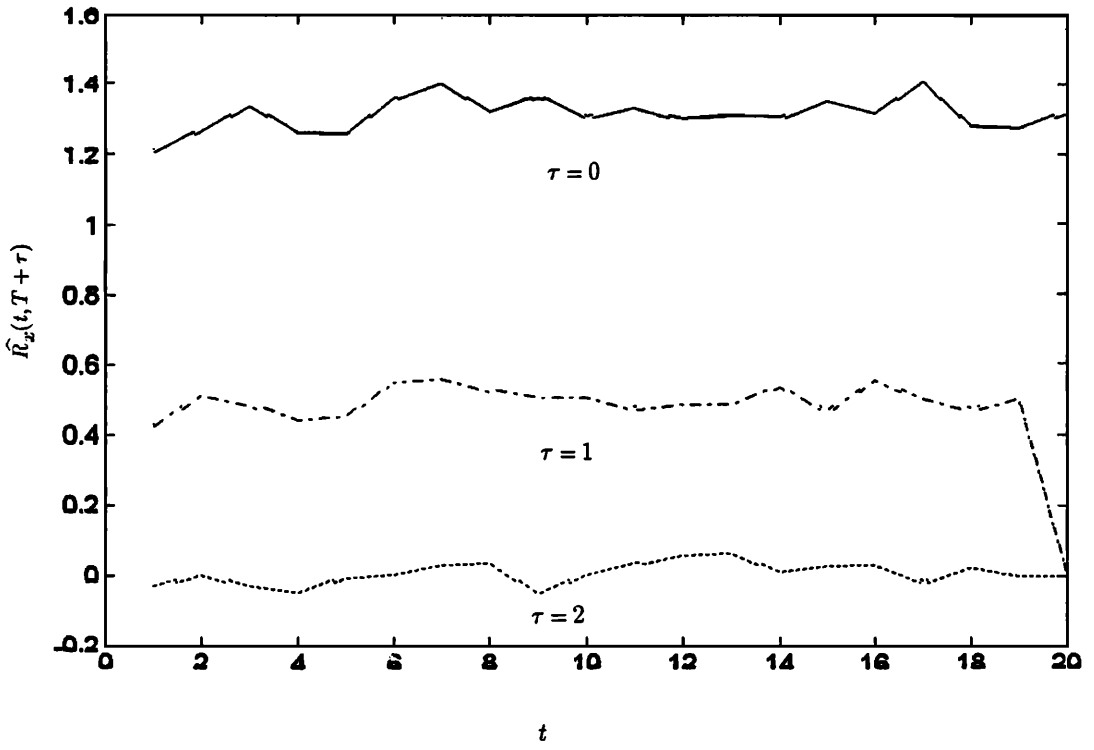

FIG. 7. Estimate of $\hat{R}_x(t,T+\tau)$ given by (5) for 30 000 points of the process defined by (9). Values of τ=0, 1, and 2.

ing average process of order one, given by

$$x(t)=h(t,0)u(t)+h(t,1)u(t-1), \tag{9a}$$

where

$$h(t,0)=1.0 \quad \text{and} \quad h(t,1)=0.5+0.4\cos[t\Omega(t)] \tag{9b}$$

and where $\Omega(t)$ is a white noise process which is distributed uniformly over the interval $[2\pi/20\pm0.03]$. Then the autocorrelation estimate (5) obtained using 10 000 data points and an assumed period $T=20$ is shown in Fig. 7, as are the values predicted by (8c).

VI. ADAPTIVE TONE SUPPRESSION

The diesel data analysis up to this point has highlighted two issues that must be addressed in order to have any chance of extracting periodic spectral information with any real temporal structure from the diesel data. One is that inaccurate period estimates, when used with long enough data lengths, will smear any time-varying spectral structure into a time-invariant structure. The period correction method proposed in Sec. V will improve matters if the interval over which the shaft period can assume to be constant is long enough to obtain statistically reliable spectral estimates, and if this period can be estimated with sufficient accuracy. The second, which is addressed in this section, is that tones with any strength must be removed in order to highlight the time-periodic spectral structure of the data. Since there can be little doubt that the shaft period is slowly time varying to some extent, it is not likely that tone cancellation assuming a fixed period will work. Our approach, therefore, is to track the tone information (magnitude, frequency, and phase) and adaptively remove it. This is attempted by using an extended Kalman filter (EKF).

In this work the EKF functions as an adaptive filter by estimating and tracking the frequency, phase and amplitude of the sinusoids and removing them from the data. Frequency estimation is a nonlinear problem, and as such, optimal filters generally cannot be constructed. The EKF arises from a linearization approach which is described in Ref. 18. The amplitude, $a_t^{(j)}$, and frequency, $\omega_t^{(j)}$, of the jth identified tone are modeled as random walk processes:

$$\omega_{t+1}^{(j)}=\omega_t^{(j)}+u_t^{(j)}, \tag{10a}$$

$$a_{t+1}^{(j)}=a_t^{(j)}+v_t^{(j)}, \tag{10b}$$

where $u_t^{(j)}$ and $v_t^{(j)}$ are uncorrelated zero mean Gaussian white noise processes with variances $\sigma_u^{(j)2}$ and $\sigma_v^{(j)2}$, respectively. Thus, the EKF-based model for the data is

$$x_t=s_t+n_t=\sum_{j=1}^{m} a_t^{(j)}\cos(\phi_t^{(j)})+n_t, \tag{11a}$$

where the phase, $\phi_t^{(j)}$, is modeled as

$$\phi_{t+1}^{(j)}=\phi_t^{(j)}+\omega_t^{(j)}+v_t^{(t)}. \tag{11b}$$

In this work, the nontonal component, $n(t)$, of the data model (11a) is assumed to be a Gaussian white noise process with variance σ_n^2. This assumption, while clearly contrary to our desire to characterize it as a periodic random process, simplifies the EKF development significantly. Moreover, for large signal-to-noise ratio (SNR) settings it is a standard assumption which can prove valuable.

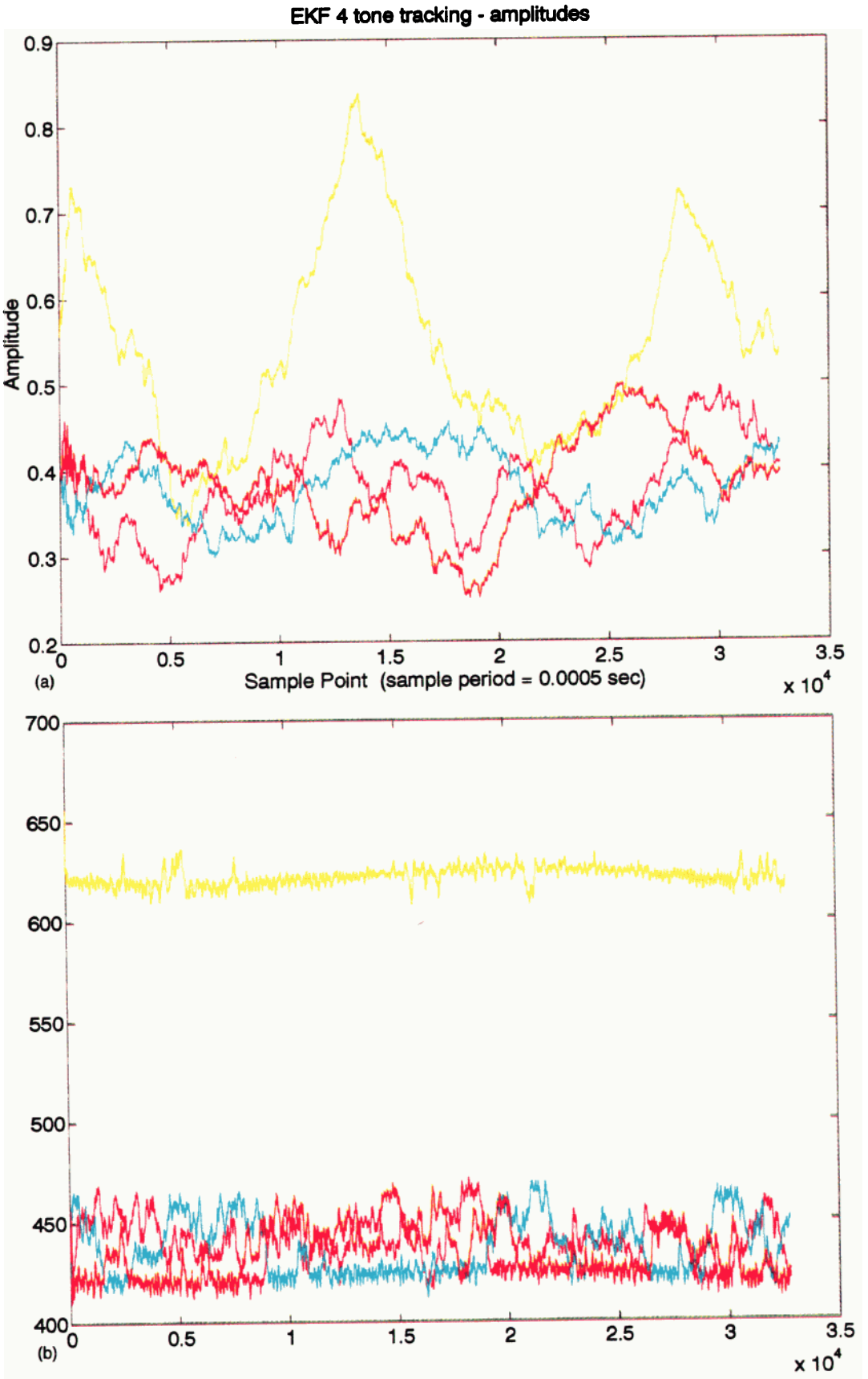

FIG. 8. EKF-based tracking estimates of the (a) amplitudes $\{a_i^{(j)}\}_{j=1}^4$ and (b) frequencies $\{\omega_i^{(j)}\}_{j=1}^4$ of the time-varying tone signal model defined in (11).

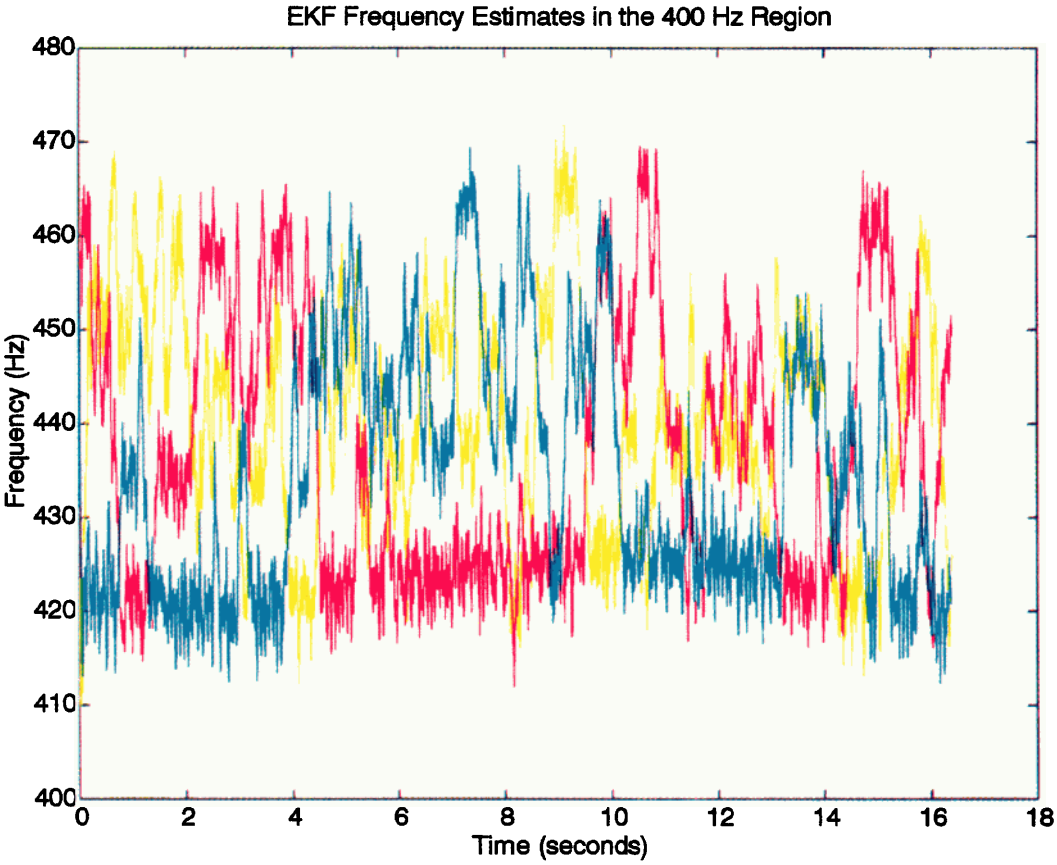

FIG. 9. Expanded version of the tracking frequencies given in Fig. 8(a).

The EKF produces approximate conditional mean filtered estimates, $\hat{a}_{t|t}^{(j)}$, $\hat{\omega}_{t|t}^{(j)}$, and $\hat{\phi}_{t|t}^{(j)}$ of the amplitude, frequency, and phase, respectively, of each jth component, and estimates the total tonal component in (11a) as

$$\hat{s}_t = \sum_{j=1}^{m} \hat{a}_{t|t}^{(j)} \cos(\hat{\phi}_{t|t}^{(j)}), \tag{12a}$$

where

$$\hat{\phi}_{t+1}^{(j)} = \hat{\phi}_{t|t}^{(j)} + \hat{\omega}_{t|t}^{(j)}. \tag{12b}$$

The full EKF equations are listed in Appendix B. These equations require initialization by supplying means and covariances for initial state estimates. These need to be chosen carefully. Otherwise, the filter may fail to estimate the tones correctly, or indeed may become unstable. The EKF is based on a Gaussian distribution assumption for the state variables, so that these initial estimates define a prior distribution on the states. As such, the information used to initialize the EKF (such as the MV estimates of the tones for amplitude and frequency) specifies these quantities. Also, as noted above, the EKF is derived in this work under the assumption that the observation "noise," n_t, in (11a) is white; whereas in this problem, this quantity consists of white measurement noise (ideally) together with the desired WCS signal. The robustness of the EKF under these conditions is currently being studied. Very little is known about its performance under these conditions. We make the point however, that for this application it performed the tone suppression task effectively, as can be seen from the diesel data results now presented.

Four tones ($m=4$) were chosen for use in the EKF tone model in (11a). Their initial values were obtained from the DFT spectrum in Fig. 1 and the MV spectra in Fig. 3. They are identified by arrows in Fig. 1. The choice to include these tones was based on the predominant time-invariant structure of the spectral data in the 400- and 600-Hz regions of Fig. 6. The initial phases $\{\hat{\phi}_{0|-1}^{(j)}\}_{j=1}^{4}$ were selected from a uniform distribution over $[-\pi,\pi]$. The tone amplitude and frequency tracking results are shown in Fig. 8. An expanded version of the frequency tracking data in the 400-Hz region is given in Fig. 9. Of particular interest are the relatively constant frequency tracks in the 420- and 620-Hz regions. The 420-Hz track corresponds to the fourth cylinder harmonic, but the track at 620 Hz is 10 Hz less than the sixth cylinder harmonic at 630 Hz. Based on this constant frequency nature, a study of the spectral data contained in the DFT spectrum in Fig. 1, and the discussion of Sec. III related to the convergence tendencies in the 400- and 600-Hz regions, we believe that these regions include system resonances which are being excited in part by tonal components. It is interesting to note that the amount of frequency variation in the EKF frequency tracked in the 420-Hz region corresponds to approximately 1 mph of variation in the vehicle speed, which is what was observed on the speedometer.

The spectral structure of the time-varying tone model, s_t, in (11a) is shown in the DFT power spectral estimate of

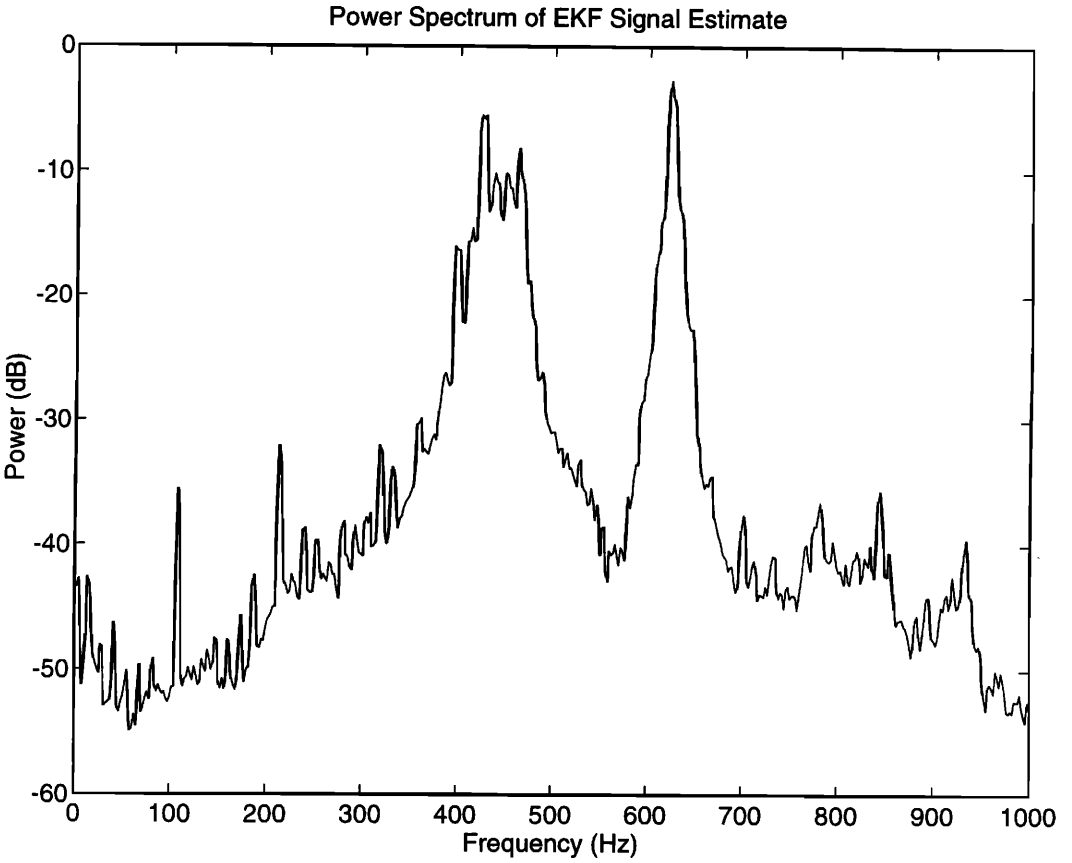

FIG. 10. DFT-based power spectrum estimate of the tone signal estimate (12) using the tracking estimates in Fig. 8.

Fig. 10. A comparison of Figs. 1 and 10 reveals that a significant amount of the data spectral structure has been accounted for by the EKF-based signal model. It should be remembered that, because of the time-varying nature of the sinusoids in this model, one should not be at all surprised that the corresponding spectral estimate contains energy over a continuum of frequencies.

The periodic time/frequency spectral estimate of the residual of the EKF operation is shown in Fig. 11. The data used to obtain this estimate were period corrected in the same way as that the original data were to arrive at Fig. 6. The first thing to note in a comparison of these two figures is the amplitude reduction achieved by the EKF. This is consistent with the effectiveness of the EKF reflected in the above comparison between the DFT spectra in Figs. 1 and 10. The contour plots in these figures are particularly helpful in assessing the influence of the EKF in the 400- and 600-Hz regions. In the 400-Hz region the EKF resulted in enhancement of the stronger spectral energy in the time interval (0.025, 0.040). A similar enhancement is observed in the 600-Hz region in the time intervals (0.010, 0.015) and (0.065, 0.070). An overall reduction of the time-invariant spectral structure in this region is also shown.

VII. SUMMARY AND CONCLUSIONS

The goal of this work was to investigate the potential value of a combination of advanced signal processing tools for extracting periodically time-varying spectral information from a complex real world system; namely vibration data measured from a diesel engine operating at nominally constant speed. A first problem that was encountered was the identification of a noninteger period, whereas digital processing demands an integer-valued period. This problem was accommodated by a simple period adjustment scheme. The value of this scheme was obvious in a simple simulation, but was not so obvious when applied to the vibration data. A second degrading influence of period uncertainty on time-varying spectral structure was noted in a theorem which states that period fluctuations can have the same temporal smearing effect as period bias if sufficiently long data sets are utilized. Unfortunately, long data sets are needed to improve statistical stability of the spectral estimate. A second problem was the dominance of the periodic time/frequency spectral estimate by relatively time-invariant tones. To separate the tone influence, and hence obtain a better picture of the time-varying spectral structure, an extended Kalman filter (EKF) was implemented to track tones in specified frequency regions. When applied to the diesel engine vibration data, the EKF resulted in a slowly time-varying tone model which was able to account for a significant amount of the energy in the data. This, in turn, resulted in some observable enhancement of the temporal structure of the vibration data spectral structure. Unfortunately, it did not improve matters enough to clearly identify temporally separate the spectral content associated with individual cylinders. This could be a shortcoming of the analysis method; in particular, the smear-

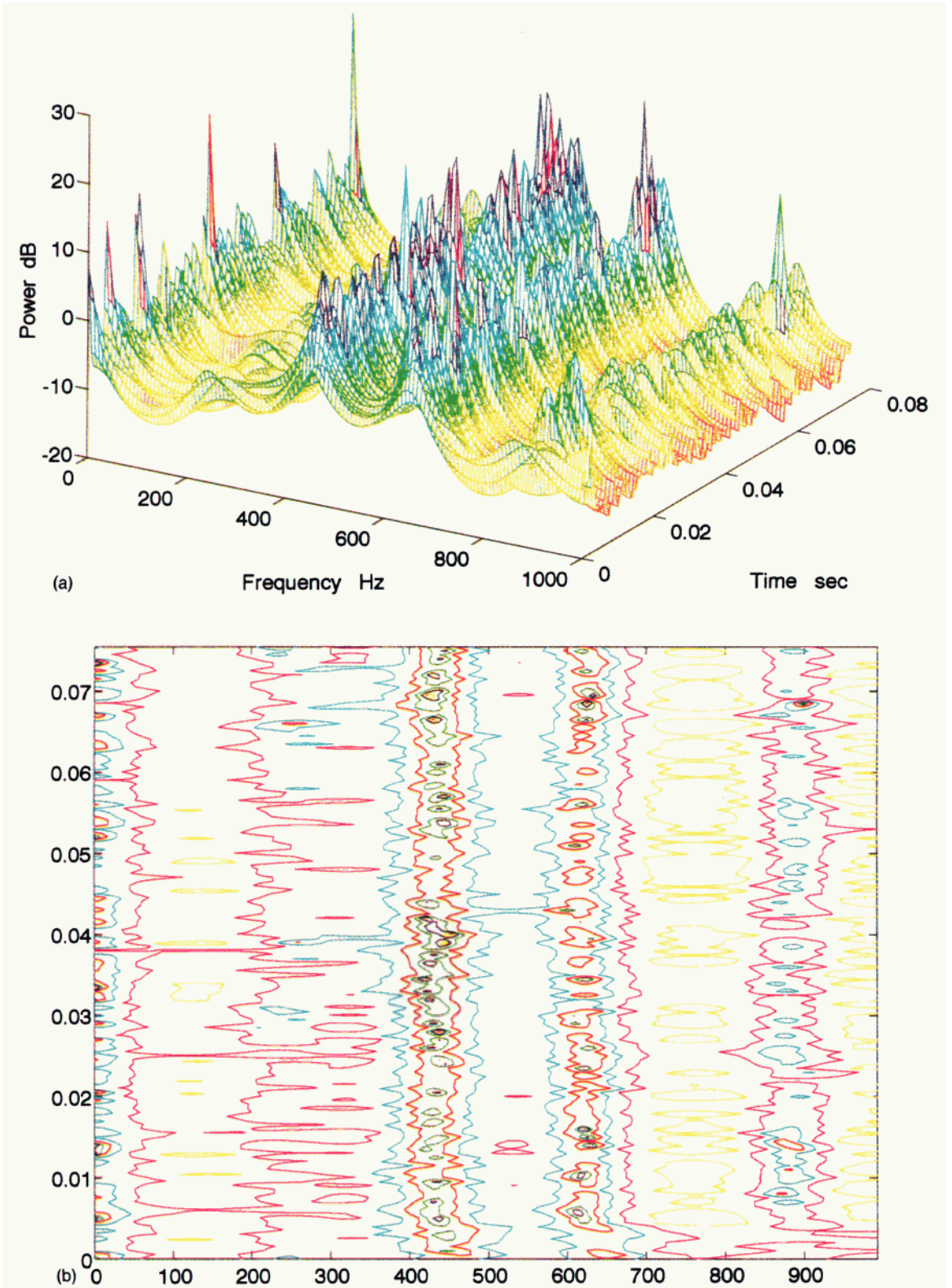

FIG. 11. AR(10) periodic spectrum estimate of the diesel data residual after removing the EKF-based tone signal estimate. (a) 3-D plot, (b) contour plot.

ing effect of period uncertainty. Or, it could be that the structural dynamics of the diesel engine were such that the cylinder responses were blended at the measurement site.

Assuming the diesel data used in this analysis are at all representative of dynamic signals associated with rotating machinery, then it is not surprising that the assumption of a wide sense stationary structure, as reflected in traditional spectral, has been so popular. This assumption however, is equivalent to assigning a uniform distribution over $[0,T]$ to time $t=0$, corresponding to the starting time for any measurement record.[12] Often, this timing information is directly available, or can be extracted (as was the case in this work).

In this case, even though the signal stochastic structure appears to be quite complex, it is reasonable to believe that some periodic spectral structure may exist, and that knowledge of that structure might provide significantly more insight into the intracycle behavior of the signal than knowledge obtained from traditional spectral methods. This belief was the premise of this work. Even though the signal processing tools chosen for this purpose did not extract obvious intracycle spectral information related to the diesel vibration signal, it is believed that enough time-varying information was sufficiently enhanced to motivate further efforts along these lines. Examples of such efforts might be inclusion of a wide sense cyclostationary structure in the EKF. The EKF used in this work assumed the nontone process to be white. Even so, it performed reasonably well in a very nonwhite and in fact nonstationary noise environment. It may also be worth investigating the influence of more accurate initial tone parameter estimates on the convergence rate of the EKF. For example, in Ref. 6 a method for improved tone amplitude estimation using the MV spectra is given. Related more directly to the MV spectra are a number of issues. The influence of slowly time-varying tones which are not true sinusoids on the rate of convergence of the MV (n) spectra could also be addressed, since, in reality, true tones do not exist.

Finally, it should be noted that the investigation provided some insight into diesel engine vibration. In particular, it showed relatively unambiguously that this vibration has a significant tonal component to it, but *not* at every harmonic of the shaft or cylinder frequency, as is often presupposed in DFT-based spectral analysis. In that or any other type of traditional spectral analysis there is always some amount of ambiguity regarding which spectral peaks correspond to tones, and which correspond to randomly excited resonances. The MV approach applied in this work revealed that only a relatively small number of harmonics contained tones of any strength. The investigation also led to the separation of this tonal structure from the remaining random structure, which suggested that structural resonances excited by random sources are present. These findings could be useful for identifying the vibration sources, and for design of noise and vibration feedback control systems. With respect to system identification for example, it is shown in Ref. 8 that if not properly accommodated, tones can introduce significant errors in attempting to perform system identification.

ACKNOWLEDGMENTS

The authors acknowledge the support of the Australian government through the Cooperative Research Centres Program and the Department of Defence. It was also supported, in part, by U.S. AFOSR Grant No. F49620-95-1-0090.

APPENDIX A: PROOF OF THE THEOREM

$$x(t)=\sum_{k=0}^{m} a_k(t)u(t-k); \quad u(t)\sim \text{WSS}, \tag{A1}$$

$$\hat{R}(t,t+\tau)=\frac{1}{N}\sum_{n=0}^{N-1} x(t+nT)\bar{x}(t+\tau+nT). \tag{A2}$$

Substituting (A1) into (A2) gives

$$\hat{R}(t,t+\tau)=\frac{1}{N}\sum_{n=0}^{N-1}\left(\sum_{k=0}^{m} a_k(t+nT)u(t+nT-k)\right)\times\left(\sum_{l=0}^{m}\bar{a}_l(t+\tau+nT)\bar{u}(t+\tau+nT-k)\right). \tag{A3}$$

Taking the expectation of (A3) yields

$$E[\hat{R}(t,t+\tau)]=\frac{1}{N}\sum_{n=0}^{N-1}\sum_{k=0}^{m}\sum_{l=0}^{m} E[a_k(t+nT)\times\bar{a}_l(t+\tau+nT)]R_u(\tau+k-l). \tag{A4}$$

Suppose

$$a_k(t)=\sum_{q=-\gamma}^{\gamma}\alpha_{kq}e^{itq\Omega(t)}; \tag{A5}$$

where $\Omega(t)$ is strongly stationary (second order), with

$$\Pr[\Omega(s)\leq w_1 \quad \text{and} \quad \Omega(t)\leq w_2]=F_\Omega(w_1,w_2;t-s). \tag{A6}$$

Then, using (A5) and (A6) the rightmost expectation in (A4) becomes

$$E[a_k(t+nT)\bar{a}_l(t+\tau+nT)]=\sum_{q=-\gamma}^{\gamma}\sum_{r=-\gamma}^{\gamma}\alpha_{kq}\bar{\alpha}_{lr}\cdot\int\int_{\Omega} e^{i[(t+nT)q\xi-(t+\tau+nT)r\delta]}dF(\xi,\delta;\tau). \tag{A7}$$

Substituting (A9) into (A4) gives

$$E[\hat{R}(t,t+\tau)]=\frac{1}{N}\sum_{n=0}^{N-1}\sum_{k=0}^{m}\sum_{l=0}^{m}\sum_{q=-\gamma}^{\gamma}\sum_{r=-\gamma}^{\gamma}\alpha_{kq}\bar{\alpha}_{lr}\cdot\int\int_{\Omega} e^{it(q\xi-r\delta)}e^{-i\tau r\delta}e^{inT(q\xi-r\delta)}\times dF(\xi,\delta;\tau)R_u(\tau+k-l). \tag{A8}$$

Define

$$f_N^{q,r}(\xi,\delta)=\frac{1}{N}\sum_{n=0}^{N-1} e^{inT(q\xi-r\delta)}. \tag{A9}$$

Then the finite summations and (A9) allow (A8) to be expressed as

$$E[\hat{R}(t,t+\tau)]=\sum_{k=0}^{m}\sum_{l=0}^{m}\sum_{q=-\gamma}^{\gamma}\sum_{r=-\gamma}^{\gamma}\alpha_{kq}\bar{\alpha}_{lr}R_u(\tau+k-l)\cdot\int\int_{\Omega} e^{it(q\xi-r\delta)}e^{-i\tau r\delta}f_N^{q,r}(\xi,\delta)\times dF(\xi,\delta;\tau). \tag{A10}$$

The functions defined by (A9) have the property

$$\lim_{N\to\infty} f_N^{q,r}(\xi,\delta)=\begin{cases}1 & \text{for } q\xi-r\delta=0\\ 0 & \text{otherwise.}\end{cases} \tag{A11}$$

Now, if $r\neq 0$ then (A11) holds on the line in $\mathbb{R}^2$ described by $\delta=(q/r)\xi$ which has Lebesque measure zero. So, assuming dF_Ω is absolutely continuous with respect to Lebesque measure, then for all $r\neq 0$ the double integral in (A10) equals zero. The same applies for all $q\neq 0$. Thus, only the $q=r=0$ terms in the appropriate summations in (A10) are retained, yielding in the limit

$$\lim_{N\to\infty} E[\hat{R}(t,t+\tau)]=\sum_{k=0}^{m}\sum_{l=0}^{m}\alpha_{k0}\bar{\alpha}_{l0}R_u(\tau+k-l). \tag{A12}$$

Special case of $u(t)\sim$iid $N(0,\sigma_u^2)$:

$$\lim_{N\to\infty} E[\hat{R}(t,t+\tau)]=\sum_{k=0}^{m}\sum_{l=0}^{m}\alpha_{k0}\bar{\alpha}_{l0}\sigma_u^2\delta(\tau+k-l)$$

$$\triangleq\mathscr{R}(\tau), \tag{A13}$$

where $\delta(\cdot)$ is the Kronecker delta function. Thus (A13) shows that as $N\to\infty$, the correlation estimate under frequency variation converges to a correlation function of some wss process.

In particular,

$$\mathscr{R}(0)=\sum_{k=0}^{m}\sum_{l=0}^{m}\alpha_{k0}\bar{\alpha}_{l0}\sigma_u^2\delta(k-l)=\sum_{k=0}^{m}|\alpha_{k0}|^2\sigma_u^2$$

and

$$\mathscr{R}(1)=\sum_{k=0}^{m-1}\alpha_{k0}\bar{\alpha}_{(k+1)0}\sigma_u^2.$$

APPENDIX B: EXTENDED KALMAN FILTER EQUATIONS FOR MULTIPLE TONE SUPPRESSION

Consider the model (10), (11). Application of the EKF equations[18] yields the following filtered estimates for the frequency, phase and amplitude of the jth tone:

$$\begin{aligned}\hat{\omega}_{t|t}^{(j)}&=\hat{\omega}_{t|t-1}^{(j)}+K_t^{(j)}\epsilon_t,\\ \hat{\phi}_{t|t}^{(j)}&=\hat{\phi}_{t|t-1}^{(j)}+L_t^{(j)}\epsilon_t,\\ \hat{a}_{t|t}^{(j)}&=\hat{a}_{t|t-1}^{(j)}+M_t^{(j)}\epsilon_t,\end{aligned} \tag{B1}$$

where ϵ_t is the signal prediction error

$$\epsilon_t=x_t-\sum_{j=1}^{N}\hat{a}_{t|t-1}^{(j)}\cos\hat{a}_{t|t-1}^{(j)}. \tag{B2}$$

The gain terms in (B1) are computed from

$$K_t=\frac{\Sigma_{t|t-1}H_t}{H_t^T\Sigma_{t|t-1}H_t}, \tag{B3}$$

where

$$K_t=[K_t^{(1)},L_t^{(1)},M_t^{(1)},\ldots,K_t^{(N)},L_t^{(N)},M_t^{(N)}]^T \tag{B4}$$

and

$$H_t=[0,-\hat{a}_{t|t-1}^{(1)}\sin\hat{\phi}_{t|t-1}^{(1)},\cos\hat{\phi}_{t|t-1}^{(1)},\ldots,0,$$
$$-\hat{a}_{t|t-1}^{(N)}\sin\hat{\phi}_{t|t-1}^{(N)},\cos\hat{\phi}_{t|t-1}^{(N)}]^T. \tag{B5}$$

The approximate error covariance matrices are updated via

$$\Sigma_{t|t}=(I-K_tH_t^T)\Sigma_{t|t-1}. \tag{B6}$$

The one-step predicted values for the next time, which are required to complete the specification of the EKF are

$$\begin{aligned}\hat{\omega}_{t+1|t}^{(j)}&=\hat{\omega}_{t|t}^{(j)},\\ \hat{\phi}_{t+1|t}^{(j)}&=\hat{\phi}_{t|t}^{(j)}+\hat{\omega}_{t|t}^{(j)},\\ \hat{a}_{t+1|t}^{(j)}&=\hat{a}_{t|t}^{(j)}.\end{aligned} \tag{B7}$$

The error covariance terms are updated as

$$\Sigma_{t+1|t}=A\Sigma_{t|t}A^T+Q, \tag{B8}$$

where

$$A=\text{bl diag}(F,\ldots,F),$$

$$F=\begin{bmatrix}1&0&0\\1&1&0\\0&0&1\end{bmatrix} \tag{B9}$$

and

$$Q=\text{bl diag}(G_1,\ldots,G_n),$$

$$G_j=\begin{bmatrix}\sigma_\omega^{(j)2}&\sigma_{\omega\phi}^{(j)}&0\\ \sigma_{\omega\phi}^{(j)}&\sigma_\phi^{(j)2}&0\\ 0&0&\sigma_a^{(j)2}\end{bmatrix}. \tag{B10}$$

The equations must be initialized with suitable values for $\hat{\omega}_{0|-1}^{(j)}$, $\hat{\phi}_{0|-1}^{(j)}$, $\hat{a}_{0|-1}^{(j)}$, $j=1,\ldots,N$ and associated error covariances $\Sigma_{0|-1}$. These values define the value and quality of the initial tone parameter estimates. The other parameters which need to be chosen are the state driving noise covariances for each signal. These values define how much these quantities can vary over time.

[1] W. A. Gardner, *Statistical Spectral Analysis* (Prentice-Hall, Englewood Cliffs, NJ, 1988).

[2] H. Tonosaki, T. Summers, H. Yamashita, and T. Nakada, "Investigations into the excitation of low frequency half order vibrations in a diesel passenger car powertrain," in *Proceedings of the Noise & Vibration Conference*, Traverse City, MI, 10–13 May 1993, pp. 339–349.

[3] *Mechanical Signature Analysis*, edited by S. Braun (Academic, New York, 1986).

[4] C. Foias, A. E. Frazho, and P. J. Sherman, "A new approach for determining the spectral data of multichannel harmonic signals in noise," Math. Contr. Signals Syst. **3**, 31–43 (1990).

[5] A. E. Frazho and P. J. Sherman, "On the convergence of the minimum variance spectral estimator in nonstationary noise," IEEE Trans. Inf. Theory **37**(5), 1457–1459 (September 1991).

[6] P. J. Sherman and K. N. Lou, "On the family of ML spectral estimates for mixed spectrum identification," IEEE Trans. Acoust. Speech Signal Process. **39**(3), 644–655 (March 1991).

[7] J. Capon, "High-resolution frequency-wavenumber spectrum analysis," Proc. IEEE **57**, 1408–1418 (1969).

[8] K. N. Lou, P. J. Sherman, and D. E. Lyon, "System identification and coherence analysis in the presence of a harmonic signal," Mech. Syst. Signal Process. **7**(1), 13–27 (1993).

[9] D. E. Lyon and P. J. Sherman, "Practical issues concerning the family of multichannel MV spectra for recovery of point spectrum," IEEE Trans. Acoust. Speech Signal Process. **41**(11), 3177–3182 (November 1993).
[10] *Cyclostationarity in Communications and Signal Processing*, edited by W. Gardner (IEEE, New York, 1994).
[11] M. Pagano, "On periodic and multiple autoregressions," Ann. Stat. **6**, 1310–1317 (1978).
[12] H. Ogura, "Spectral representation of a periodic nonstationary random process," IEEE Trans. Inf. Theory **17**(2), 143–149 (March 1971).
[13] Q. Zhuge, Y. Lu, and S. Yang, "Non-stationary modeling of vibration signals for monitoring the condition of machinery," Mech. Syst. Signal Process. **4**(5), 355–365 (1990).
[14] J. C. Hardin and A. G. Miamee, "Correlation autoregressive processes with application to helicopter noise," J. Sound Vib. **142**(2), 191–202 (February 1990).
[15] A. M. Yaglom, *Correlation Theory of Stationary and Related Random Functions* (Springer-Verlag, New York, 1987).
[16] G. J. Adams, "Parameter estimation for systems with periodic components," Ph.D. dissertation, Department of Electrical Engineering, The University of Newcastle, NSW, Australia (12 February 1994).
[17] L. S. Marple, *Digital Spectral Analysis with Applications* (Prentice-Hall, Englewood Cliffs, NJ, 1987).
[18] B. D. O. Anderson and J. B. Moore, *Optimal Filtering* (Prentice-Hall, Englewood Cliffs, NJ, 1979).
[19] A. G. Miamee and J. C. Hardin, "On a class of nonstationary stochastic processes," Sankhyā: Indian J. Stat., Ser. A **52**(2), 145–156 (1990).